Covariability of Spring Snowpack and Summer Rainfall across the Southwest United States

DAVID S. GUTZLER

Department of Earth and Planetary Sciences, University of New Mexico, Albuquerque, New Mexico

(Manuscript received 18 October 1999, in final form 29 February 2000)

ABSTRACT

Interannual fluctuations of observed summer rainfall across the monsoon region of the southwestern United States are analyzed to ascertain their spatial coherence and to test the hypothesis that antecedent spring snowpack anomalies may modulate the monsoon and exhibit an inverse correlation with summer rainfall anomalies. To characterize the spatial coherence of seasonal rainfall anomalies, an objective linear analysis of interannual variability is applied to climate divisional data across the Southwest. Three coherent subregions are identified, broadly representing rainfall anomalies across Arizona, eastern New Mexico/western Texas (the Southwest Plains), and most of New Mexico. Interannual fluctuations of summer rainfall in the New Mexico region exhibit a very significant negative correlation with a large-scale index of the antecedent 1 April snowpack over the southern U.S. Rocky Mountains during the 1961–90 climatic averaging period. This strong relationship seems to break down in the years before and after this period, possibly indicating a shift in climate associated with other forcing factors.

1. Introduction

For more than a century, meteorologists have attempted to establish predictive schemes for the Southeast Asian summer monsoon. Monsoonal climate regimes, characterized by wet summers and dry winters, are seasonally reversing thermally direct circulations in which warm (less dense) air rises and cold (more dense) air sinks. Monsoons occur over continental areas close enough to low-latitude oceans that the difference in heat capacities between land and ocean is sufficient to create a seasonal reversal in the land–ocean temperature gradient, driving a moist onshore flow in summer and a dry offshore flow in winter.

Thus, one potential way to modify the strength of the summer onshore flow is via the lingering effects of snow cover on the rate of continental surface heating (Hahn and Shukla 1976). In years of heavy late-season snow cover, the continental pole of a thermally direct monsoonal circulation may generate less surface heating for the overlying atmosphere than is the case in ''normal'' years, and the ensuing summer monsoon is weak; similarly years of light snow cover should be followed by strong summer monsoons. The seasonal lag inherent in this scenario has, for over a century (beginning with Blanford 1884), motivated the examination of spring snowpack as a possible mechanism for monsoon prediction.

According to this hypothesis, summer precipitation is controlled primarily by the static stability of the atmosphere and can be enhanced or suppressed dynamically via surface heating anomalies. The memory of snowpack anomalies for monsoonal circulations can be thought of as a large-scale negative feedback on the climate system, since wet winters lead to dry summers and dry winters lead to wet summers. The feedback is nonlocal because the area of snowpack forcing is generally not the same as the area of summer rainfall response (Barnett et al. 1989).

There is limited supporting evidence for surface moisture to exert an inverse control on precipitation in recent model-based research. The importance of land surface forcing on monsoon intensity, relative to oceanic variability or atmospheric dynamical factors, is still an active topic of Asian monsoon research (Yang et al. 1996; Yang and Lau 1998; Kripalani and Kulkarni 1999). Paegle et al. (1996) showed that increased evaporation in summer in the middle United States could suppress moist inflow from the Gulf of Mexico and thereby suppress precipitation.

This paper presents empirical evidence that an inverse spring snow–summer rainfall relationship as described above can be found in data from the southwestern United States. A preliminary study of the northern fringe of the North American monsoon system suggested the ex-

Corresponding author address: Dr. David S. Gutzler, Earth and Planetary Sciences Dept., University of New Mexico, Albuquerque, NM 87131-1116.
E-mail: gutzler@unm.edu

istence of a weakly significant correlation between the average spatial coverage of spring snow across the U.S. Rocky Mountain region, and subsequent summer rainfall averaged over the state of New Mexico (Gutzler and Preston 1997). That study was limited by the arbitrary choices of snow cover and precipitation indices, the short period of record of the satellite-derived spring snow index, and the possible mixing of decadal trends with shorter-term interannual fluctuations.

To address those limitations, this paper presents separate analyses of summer precipitation and spring snowpack, based on datasets of longer duration, that are designed to describe the spatial variability of snow and rainfall, distinguishing between multidecadal and subdecadal fluctuations. From such analyses objective indices of spring snow and summer rainfall are defined, which then are used to explore the existence of an inverse lag relationship between spring snow and summer rainfall in the Southwest. The patterns of interannual summer rainfall variability are themselves of interest: three distinct subregions are identified, suggesting that the relative importance of different physical mechanisms modulating seasonal rainfall may vary across the Southwest monsoon region.

Whether the climate of Southwest North America can be appropriately described as monsoonal at all has been debated for some years (Adams and Comrie 1997) because there is no true large-scale seasonal wind reversal, or a clear monsoon vortex transporting copious amounts of water vapor in the boundary layer, such as are obvious in southern Asia. However recent analyses have shown local evidence in southern Arizona for a wind reversal (Douglas et al. 1993), and the transport of moisture into the southwest United States at both near-surface and midtropospheric levels has been diagnosed by Schmitz and Mullen (1996). Furthermore Higgins et al. (1997) demonstrated the existence throughout the Southwest of an identifiable ''onset date'' of the summer rainy season, another characteristic of monsoonal climates. These studies have examined the spatial coherence and mean seasonal variability of North American summer precipitation.

For our purposes we seek to ascertain the spatial coherence of year-to-year variability of summer rainfall in order to test the validity of a land surface forcing hypothesis applied to monsoon anomalies. To address the issue of the spatial coherence of seasonal rainfall anomalies, we apply in section 3a standard eigenfunction analysis procedure, Varimax-rotated empirical orthogonal function (REOF) analysis (Horel 1981; Richman 1986; Cayan 1996), to 45 yr of precipitation data.

Section 4 then describes the same analysis applied to spring season snowpack data. Having derived independent indices based on the principal coherent patterns of interannual spring snowpack and summer rainfall anomalies, we then demonstrate in section 5 that in recent decades an inverse snowpack–rainfall relationship exists consistent with the hypothesis developed for the Asian summer monsoon. The analysis yields a relationship stronger than previously documented by Gutzler and Preston (1997), and stronger than corresponding correlations between North American rainfall and equatorial Pacific SST. Nevertheless the predictability of summer rainfall associated with antecedent snowpack is limited, in part due to questions about the long-term robustness of the relationship.

2. Climatology of summer rainfall and spring snowpack

Precipitation data come from the cooperative observer network coordinated by the U.S. National Weather Service, and have been averaged temporally and spatially into monthly means within intrastate climate divisions defined by the National Climatic Data Center in Asheville, North Carolina. The climate divisions represent a sacrifice of spatial resolution (as could in principle be obtained from a network of individual stations) in favor of some built-in spatial averaging, potentially increasing the significance of each seasonal anomaly. We also choose to use bimonthly averages of rainfall instead of monsoon onset dates, which, arguably, could be more closely related to premonsoon surface forcing. Higgins et al. (1998) have shown, however, that anomalies of monsoon onset dates are highly correlated with summer season precipitation (early onset leading to above-average rainfall), so we anticipate that the results here would be applicable to onset dates as well.

For the present analysis 23 climate divisions have been retained, including all of Arizona and New Mexico, and parts of Utah, Colorado, and Texas. This domain extends well beyond the ''monsoonal'' region of the Southwest defined in previous studies by the sudden onset of precipitation in July (Mock 1996; Higgins et al. 1997). Precipitation for the two months of July and August (hereafter denoted JA) for each year were summed in order to describe the annual ''monsoon season'' rainfall for each division.

Figure 1a shows the mean JA rainfall for the 23 divisions for the 45-yr period from 1951–95. Maximum rainfall, exceeding 150 mm, occurs in southeastern Arizona and the central part of New Mexico. Less than 60 mm of rain falls in western Arizona and southern Utah, which lie west and north of the ''monsoon region'' defined by previous authors (e.g., Higgins et al. 1997). Rainfall reaches intermediate values (90–150 mm) in west Texas, eastern New Mexico, and southeastern Colorado; these regions also exhibit substantial spring season rains and so are typically not considered part of the southwestern summer precipitation regime (Mock 1996; Higgins et al. 1997).

The total interannual standard deviation of precipitation in these regions is depicted in Fig. 1b. Two maxima in variability are found, one in central Arizona and the other in eastern New Mexico. A distinct local minimum occurs in western New Mexico, and variability

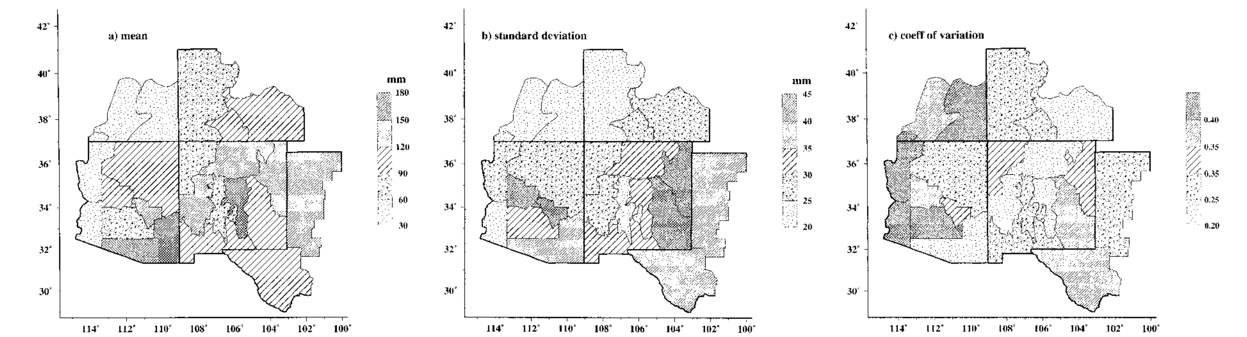

FIG. 1. (a) Mean Jul + Aug precipitation in 23 southwest United States climate divisions for the 45-yr period 1951–95 (units = mm). (b) Interannual standard deviation of Jul + Aug precipitation (units = mm). (c) Coefficient of variation (interannual standard deviation/mean) of Jul + Aug precipitation.

is relatively low across the northern tier of divisions included in the analysis domain. The interannual variability can be placed into context relative to mean rainfall via the dimensionless coefficient of variation (CoV, defined as the ratio standard deviation/mean), shown in Fig. 1c. The largest values of CoV are found in western Arizona and southern Utah where the mean is small. The core region of the American monsoonal regime in eastern Arizona and western New Mexico, as depicted by Higgins et al. (1997) for example, corresponds to the stippled divisions in Fig. 1c where the CoV attains relatively small values (less than 0.3).

Spring snow cover data are derived from manual snow course observations, reporting snow depth in terms of inches of snow water equivalent (or SWE), taken at 48 sites on or close to 1 April of each year at a network of observing sites maintained by the U.S. Natural Resources Conservation Service. Most of these sites are located in mountainous areas where snow is continuously present throughout the cold season, so interannual fluctuations of snow depth will not in general correlate directly with simultaneous fluctuations of snow-covered area. Complete time series for these sites are available for the period 1961–90, the most recent standard 30-yr climatic averaging period.

As in other studies examining the possible effects of antecedent snowpack on summer monsoons, there is considerable uncertainty as to the most appropriate index of snow to use (Barnett et al. 1989). Part of this uncertainty results from the multiplicity of ways in which snow might affect the land–sea heating contrast that we hypothesize is driving the monsoon circulation. Positive snow cover anomalies would increase the surface albedo; this effect would presumably be most pronounced when the areal extent of snow is maximized in springtime and the depth of snow in regions of heavy snowpack would be of lesser importance (Yasunari et al. 1991). Positive snow anomalies also should increase the local rates of evaporation and sublimation, allowing the surface to lose heat as insolation increases during the spring season without warming up. Even after the snow melts it could modulate the surface heat budget through the lingering effects of soil moisture anomalies.

Current observational datasets (for snow or soil moisture) are not sufficient to properly diagnose all these processes on interannual timescales. High-resolution modeling studies are currently in progress to examine a simulated surface energy budget for the North American monsoon system. Meanwhile for the present study we will use long-term indices of 1 April SWE, which have been used before as an index of late-season snowpack in the western United States for hydrological studies (e.g., Cayan 1996; Cayan et al. 1998; and many others).

Figure 2a illustrates the 30-yr mean 1 April SWE value at each site. The 30-yr mean exhibits a strong altitude dependence (not discernible from this plot since altitudes are not shown), and sites in Utah and Colorado generally exhibit larger mean snow depths than the sites in Arizona and New Mexico to the south. The interannual standard deviation of these data, shown in Fig. 2b, exhibits less overall, and less systematic, spatial variability. The coefficient of variation statistic is maximized at sites with large interannual variability relative to the mean snow depth (Fig. 2c), and by this measure the southern sites are sensitive measures of climate anomalies. Thus, despite the geographical and altitude-dependence of mean SWE, the spatial analysis of SWE anomalies should not be unduly biased a priori in favor of the regions of more mean snowfall.

3. Interannual variability of summer rainfall across the Southwest

a. Multidecadal variability

Long-term (multidecadal) trends in summer rainfall are evident in these data, as examined previously by Cayan (1996). Figure 3 shows the linear trend of JA rainfall over the period 1951–95 for each climate division. Note that the linear trend is generally positive across much of New Mexico, southern Colorado, and western Texas but negative across Arizona. For com-

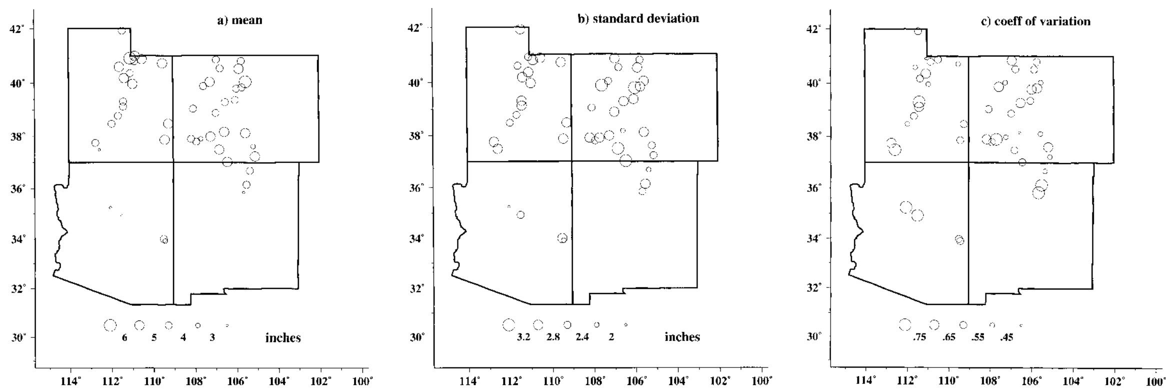

FIG. 2. (a) Mean 1 Apr snow water equivalent depth (SWE; units = in.) at 48 manual snow course sites for the 30-yr period 1961–90. (b) Interannual standard deviation of 1 Apr SWE (units = in.) (c) Coefficient of variation (interannual standard deviation/mean) of 1 Apr SWE.

parison, twentieth century trends in annual average precipitation are generally positive across this domain, especially across the southern halves of Arizona and New Mexico (IPCC 1998, Fig. 8.5).

Quantitative removal of long-term trends is difficult, because linear regressions (or other ''trend'' diagnostics) are often quite sensitive to values near the endpoints of the time series. In Arizona division 4 (east central), the mean JA rainfall in Fig. 1a is 130 mm and the ''trend'' in Fig. 3 is -0.98 mm yr^{-1}. This trend is obviously unsustainable over the long term, because a straightforward extrapolation forward in time suggests, implausibly, that summer rainfall will cease altogether in the year 2100.

Some clarification of these trends can be obtained from Fig. 4, which shows time series of JA rainfall for the entire twentieth century in Arizona division 4 (east central) and New Mexico division 5 (central valley), with quadratic curve fits shown for each time series. In both regions the first time derivative of the quadratic fit changes sign in midcentury, when rainfall in east central Arizona reaches a maximum before declining, and rainfall in the New Mexico central valley reaching a minimum before increasing during the second half-century. Clearly century-long regressions for these regions would be considerably smaller in magnitude than the corresponding 1951–95 linear regressions, with some doubt even surrounding the sign of the trends.

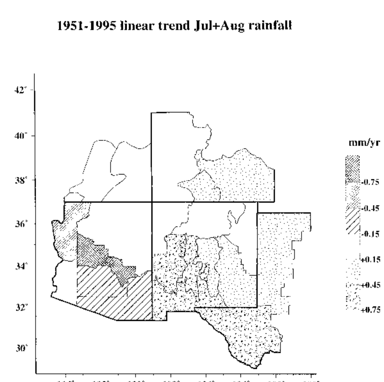

FIG. 3. Linear regression coefficient for division time series of Jul + Aug precipitation for the 1951–95 analysis period (units = mm yr^{-1}).

b. Interannual variability

The principal aim of this paper is to examine shorter-term interannual variability of summer rainfall and its possible correlation with antecedent spring snow. To characterize the spatial coherence of interannual variability of these data in an objective way, REOF analysis is employed. This analysis technique tends to draw out regional-scale coherent patterns, and we expect that the spatial loadings yielded by the analysis will be smaller in extent than unrotated EOF analyses.

For this study it would be desirable to isolate inter-

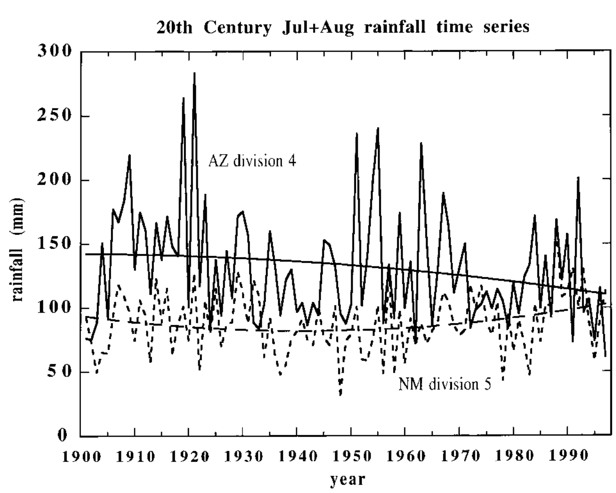

FIG. 4. Time series of Jul + Aug precipitation for two climate divisions (Arizona 4, east central, and New Mexico 5, central valley) for the entire twentieth century, shown as solid and dashed lines, respectively. Quadratic fits to the time series are shown as smoothed lines.

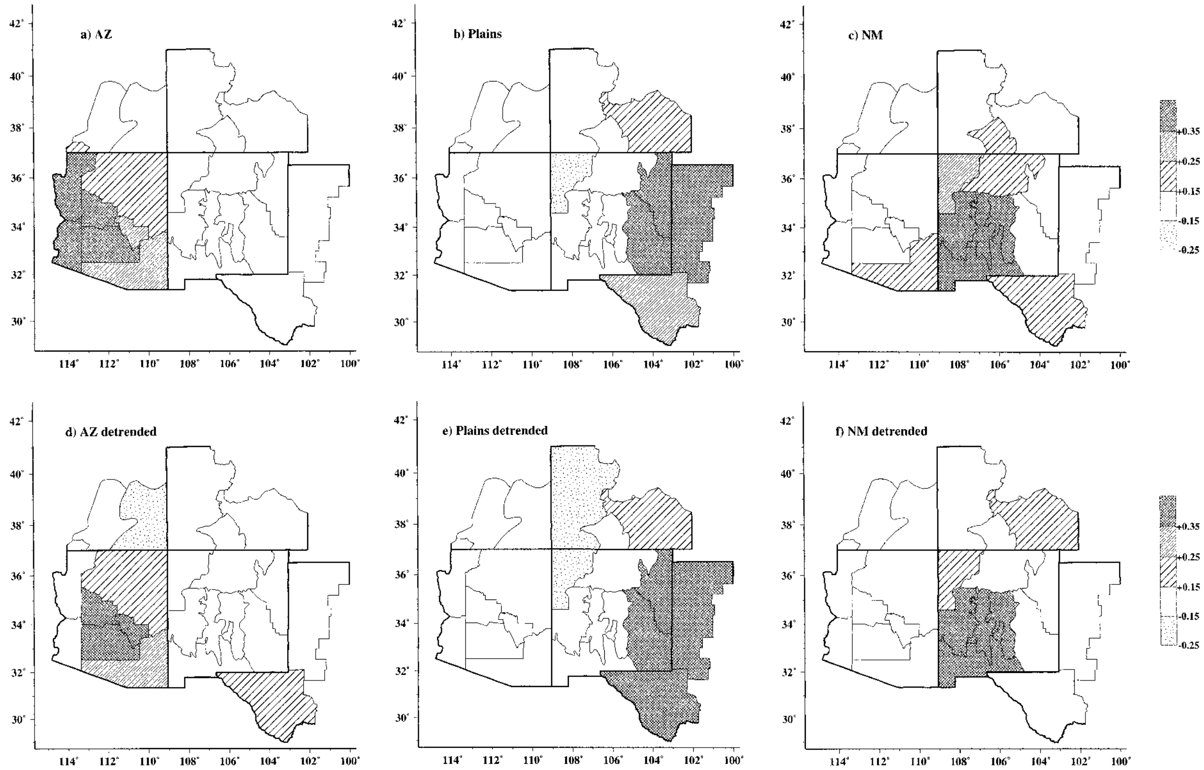

FIG. 5. Regions of coherent interannual summer (Jul + Aug) precipitation anomalies across the American Southwest, derived from Varimax-rotated empirical orthogonal function analysis applied to 45 yr of data. (a)–(c) Derived from correlation matrix of actual anomalies (trend not removed). (d)–(f) Derived from detrended anomalies. Scale for shading scheme is shown to the right of (c) and (f): in each panel, divisions with no significant loading are left blank; light hatching, dense hatching, and cross-hatching denote progressively higher positive loadings; and light stippling denotes negative loading (i.e., stippled and hatched divisions fluctuate out-of-phase). (a) Region I, Arizona (26% of total normalized variance). (b) Region II, Plains (23% of variance). (c) Region III New Mexico (19% of variance). (d)–(f) As in (a)–(c) but derived from detrended Jul + Aug precipitation time series.

annual from multidecadal variability, but as illustrated in the previous subsection there is no straightforward way to carry this out. To test the sensitivity of REOF analyses to decade-scale variability, such analyses were carried out twice on the cross-correlation matrix of the 23 divisional JA time series for the 1951–95 period. The initial analysis derived REOFs from the time series of raw interannual anomalies, with no attempt to remove multidecadal variability. In the second analysis REOFs were derived after removing the 1951–95 linear trend illustrated in Fig. 3 from each divisional time series.

In both analyses, the first two of 23 eigenvalues (not shown) accounted for considerably more variance than subsequent values, and the first five eigenvalues exceeded the value corresponding to an equal share of variance per eigenmode. The first three rotated eigenvectors were robust to changes in the number of unrotated vectors kept in the analysis, and these three patterns for each analysis are described here.

As shown in Fig. 5, the spatial loadings associated with the three largest eigenvalues in each analysis are very robust, that is, the patterns of interannual JA rainfall variability are not sensitive to the presence or absence of long-term trends in the data. That is, Fig. 5a, showing the first rotated mode with trend included, describes effectively the same spatial variability as its detrended counterpart in Fig. 5d, and so forth for the second and third rotated eigenvectors. Considering the large uncertainties in trend removal discussed in the previous subsection, we choose to focus on the unfiltered interannual REOF patterns (Figs. 5a–c) and the discussion henceforth pertains primarily to those patterns and the time series of expansion coefficients derived therefrom. When interpreting the results, however, it should be kept in mind that multidecadal variability is mixed with shorter-term fluctuations.

The REOF analysis of the cross-correlation matrix of JA rainfall values yields three principal large-scale regions (Figs. 5a–c), which independently account for 26%, 23%, and 19% of the normalized interannual rainfall variance across this domain. Thus fluctuations in these three regions together account for 68% of the total interannual rainfall variance; a marked drop-off in explained variance occurs in subsequent REOF patterns.

If summer season rainfall anomalies varied coherently across the entire Southwest, then the REOF analysis should yield a single monopolar pattern accounting for a large fraction of the total variance, projecting signif-

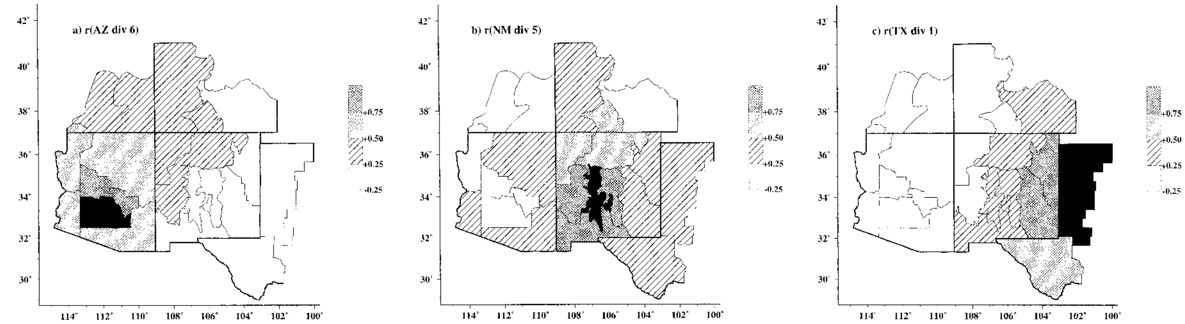

FIG. 6. Interannual Jul + Aug rainfall anomalies in a single division (shown in solid black) correlated with rainfall anomalies in all other divisions. (a) Arizona division 6. (b) New Mexico division 5. (c) Texas division 1.

icantly onto all (or at least most) climate divisions within the analysis domain. This is a good description of the structure exhibited by the EOF patterns whose Varimax rotation is described here (not shown). However the REOF analysis suggests that the subdomains delineated by the cross-hatching in the REOF patterns shown in Fig. 5 represent separable regions of spatially coherent anomalies, indicating that summer rainfall varies somewhat independently, and may therefore be independently modulated, in these regions.

Region I, denoted ''Arizona,'' includes most of Arizona extending into southwestern Utah, entirely west of the continental divide. This is the area of the analysis domain closest to the roots of the ''Mexican monsoon'' in western Mexico (Douglas et al. 1993). Carleton et al. (1990) examined interannual modulation of summer precipitation by a variety of factors, using a statewide average of cooperative sites in Arizona as their principal precipitation index. The REOF analysis suggests that such an average should be reasonably coherent, and their results should be applicable to the interannual variability of summer rainfall in region I.

Region II, denoted ''Plains,'' incorporates the easternmost area of the analysis domain, including the two climate divisions in Texas, plus the Divisions in the plains of eastern New Mexico and southeastern Colorado. Most of the subdomain covered by this region is outside the monsoonal region of North America defined from the seasonal cycle of rainfall (Mock 1996; Higgins et al. 1997). This region is entirely east of the continental divide and east of the Front Range in Colorado and the north–south mountains in New Mexico that form the eastern boundary of the Rio Grande Rift. It is likely that the preponderance of summer moisture supply to this region comes from the southeast (the Gulf of Mexico).

Region III, denoted ''New Mexico,'' is sandwiched between the first two regions, and projects most strongly onto the highlands of central and western New Mexico. This region straddles the continental divide, which runs from the New Mexico boot heel northward across the western part of the state and is not generally a prominent topographic feature. Of the three regions delineated by the REOF analysis, region III is located farthest from either of the two possible source regions for monsoonal moisture, the Gulf of California to the southwest and the Gulf of Mexico to the southeast. This region may receive a mix of moisture transported from either the southwest or the southeast (Schmitz and Mullen 1996).

Confirmation of the regional scale of JA rainfall anomalies across the southwest United States is made by examining ''one-point correlation maps'' based on individual regions at the heart of the principal spatial loadings in the REOFs. These are shown in Fig. 6 for base divisions Arizona 6, Texas 1, and New Mexico 5, corresponding to the Arizona, Plains, and New Mexico regions, respectively. In each case the correlation is high (exceeding 0.75) in most of the climate divisions immediately adjacent to the base division, but drops off to less than 0.25 in divisions farther away. The REOF patterns are only slightly more compact than the decorrelation scale suggested by the plots in Fig. 6. None of the REOF patterns or correlation maps suggest strong systematic inverse relationships (as in teleconnection patterns of geopotential height fields), in which rainfall varies inversely across the analysis domain, as would be the case if, for example, anomalously dry summers in New Mexico were associated with wet summers in Arizona.

The time series of expansion coefficients associated with these patterns are shown in Figs. 7a–c, together with time series describing SWE and Pacific SST fluctuations that will be discussed later. Visual inspection of the JA rainfall time series suggests that decadal-scale variability is more prominent than secular trends, consistent with analyses by Cayan et al. (1998). For example, the Arizona and New Mexico time series (Figs. 7a and 7c) appear to exhibit much more variability during the first and last 15 years of the data record, surrounding a period of relative quiescence between about 1965 and 1980.

The Southwest Plains were afflicted by a very severe drought in the early to mid-1950s (Namias 1955), manifested here by seven consecutive years of negative anomalies at the beginning of the Plains time series (Fig. 7b). The drought does not appear as a particularly high-

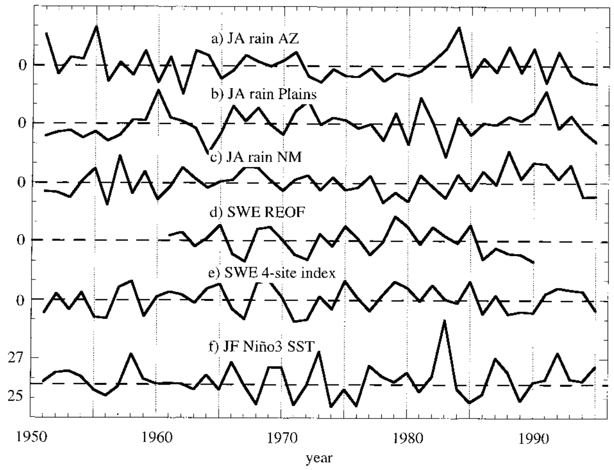

FIG. 7. Time series of summer (Jul + Aug) precipitation, spring (1 Apr) SWE, and winter (Jan + Feb) equatorial Pacific SST. All time series are nondimensional, with the exception of the SST time series in 7f. (a) Jul + Aug precipitation anomalies in Arizona, derived from Fig. 5a. (b) Jul + Aug precipitation anomalies in the Plains, derived from Fig. 5b. (c) Jul + Aug precipitation anomalies in New Mexico, derived from Fig. 5c. (d) 1 Apr SWE anomalies, derived from Fig. 8. (e) 1 Apr SWE anomalies, averaged over the four snowcourse sites listed in Table 1. (f) Jan–Feb average of Niño-3 SST (units = °C).

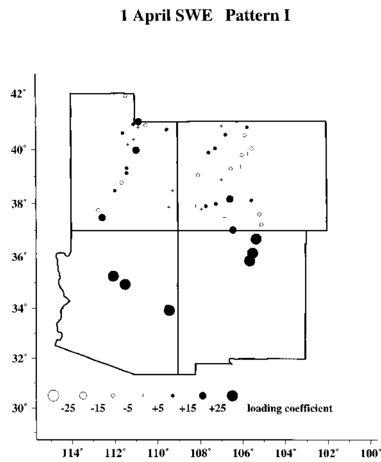

FIG. 8. The gravest pattern of spatially coherent, interannual spring (1 Apr) SWE anomalies, derived from REOF analysis of 30 yr of SWE data. Sites with no significant loading are marked by a +; solid circles represent positive loadings, with the size of the circle indicative of the loading; and open circles represent negative loadings in the same way.

amplitude event in the Plains time series, but this is the region least monsoonal in character (July and August do not account for a disproportionately large fraction of annual rainfall in the Plains region). The 1950s drought signal is progressively less apparent in summer rainfall moving westward to New Mexico (Fig. 7c) and Arizona (Fig. 7a).

4. Spring snowpack versus summer rainfall

We now ask whether the interannual variability of summer monsoonal precipitation anomalies in any of the three regions described by the REOF analysis of JA rainfall exhibits a significant relationship with antecedent spring SWE anomalies. An index of spring SWE is derived from REOF analysis of the interannual cross-correlation matrix derived from the network of snowcourse observations shown in Fig. 2.

The first REOF of normalized interannual 1 April SWE anomalies over this time period, shown in Fig. 8, accounts for 13% of the total SWE variance (more than any other pattern of SWE anomalies); this pattern also emerged as the first (unrotated) EOF mode with rotation making little difference. The largest projections onto this pattern come from sites near the southern margin of the domain, including all the sites in New Mexico and Arizona and other sites in southern Utah and Colorado. This pattern accounts for relatively little variance at sites north of latitude 38°N. Thus the southern Rockies exhibit spring snowpack anomalies that vary somewhat independently of snowpack anomalies in central and northern Utah and Colorado.

This pattern is quite similar to the New Mexico pattern of interannual variability of 1 April SWE values derived by Cayan (1996). That study indicated the tendency for positive anomalies in 1 April SWE to be followed by several months of below average surface temperature. Although cause and effect are difficult to separate, Cayan's observation is consistent with the hypothesis that the effects of enhanced snowpack may persist long enough to affect the surface heating that drives the monsoon.

Figure 7d shows the time series of expansion coefficients of the SWE REOF in Fig. 8. Some suggestion of a negative trend is implied from the observation that SWE anomalies are negative for each of the final five years (1986–90) of the time series, but no attempt to remove this trend has been made for reasons given in the following paragraph. It is easy to see an out-of-phase relationship between Fig. 7d and the time series just above it (Fig. 7c, describing summer rainfall in New Mexico), illustrating one of the principal conclusions of this paper.

To extend the snow time series to the entire period of record, Fig. 7e shows a temporally extended SWE index derived by calculating a four-site average of snow depths based on several snowcourse sites in Arizona and New Mexico with the largest spatial loadings in Fig. 8. These snowcourse sites, listed in Table 1, have complete records for the same period as the rainfall data (1951–95). Figures 7d and 7e track each other closely (but, of course, not perfectly) during the 1961–90 overlap period. Note that the apparent downward trend in the 1980s, which appears less pronounced in the four-station index than in the REOF time series, ceases after 1990, making trend removal problematic.

The scatterplot of 45 annual pairs of 1 April SWE

TABLE 1. Manual snow course sites used for the spring snowpack index illustrated in Fig. 7e. The index is derived from the four-site arithmetic mean of 1 Apr snow water equivalent depth, multiplied by 0.8 to make the amplitude of the index the same as the first REOF of 1 Apr snow depth (Fig. 7d).

Site name	Latitude (N)	Longitude (W)	Elev. (m)
Maverick Fork Pillow, AZ	33°55′	109°27′	2800
Mormon Mtn. Snow Course, AZ	34°56′	111°31′	2290
Hematite Park, NM	36°40′	105°22′	2900
Tres Ritos, NM	36°08′	105°32′	2620

anomalies and JA western New Mexico rainfall anomalies is shown in Fig. 9. Solid circles in the figure use the 30 REOF-based nondimensional SWE anomalies for the 1961–90 period. Over this time period, corresponding to the most recent standard 30-yr climatic averaging period, there was a very significant one-season lagged relationship between spring snow and summer rainfall in the expected sense, that is, deficient summer rain across western New Mexico follows heavy spring snow in the southern Rocky Mountains, and abundant summer rain follows light spring snow. The linear correlation derived from the set of solid circles is −0.61, easily significant at the 5% level (assuming each year represents 1 dof), and considerably better than the correlation derived by Gutzler and Preston (1997) based on a shorter data record. The correlations between SWE anomalies and either Arizona or Plains summer rainfall (Figs. 7a,b,d) are also negative but considerably smaller in magnitude (about −0.3).

The 15 open circles in Fig. 9 are based on the four-station 1 April SWE index for 1951–60 and 1991–95, and it is easily seen that they exhibit no significant correlation with New Mexico summer rainfall. Perhaps the lag relationship exhibited between fluctuations of SWE and western New Mexico rainfall during the 1961–90 period is not robust to longer averaging periods, either because the high correlation is the result of random chance, or because the dynamics of the climate system changed. The latter possibility is discussed further in the next section.

Alternatively, it is possible that the four-station index does not capture the large-scale snow-related surface forcing as adequately as the REOF pattern in Fig. 8. In 1995, for example, spring SWE values were well above normal across southern Colorado, but the four-station SWE index based on just Arizona and New Mexico snow course sites was negative that year, and the subsequent summer rainfall anomaly in western New Mexico was negative as well.

It is instructive to compare the magnitude of the lag correlation between spring snow and summer rainfall with the corresponding correlation between El Niño–Southern Oscillation (ENSO) indices of equatorial Pacific SST with summer rainfall in the Southwest. Most current operational seasonal forecast skill for North America is derived from ENSO-related predictability.

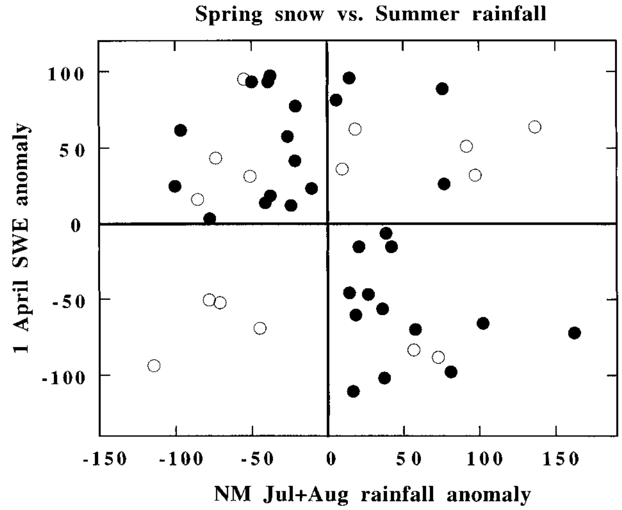

FIG. 9. Scatterplot of nondimensional values of 1 Apr SWE anomalies (from Fig. 7d and 7e) and New Mexico Jul + Aug precipitation anomalies (from Fig. 7c). Solid circles are years within the 30-yr period 1961–90 and are based on the SWE expansion coefficients in Fig. 7d. Open circles are years between 1951–60 and 1991–95 and are based on an average of four SWE sites (listed in Table 1) whose time series are shown in Fig. 7e. The linear correlation associated with the solid circles is −0.61; the open circles exhibit no correlation.

Table 2 shows the results of correlating the Niño-3 SST index (surface temperature averaged over the box delineated by 5°N, 90°W, 5°S, and 150°W) with the three JA rainfall time series shown in Figs. 7a–c. We focus on the 1961–90 period when the spring snow–summer rainfall relationship was strong; extending the analysis to a longer period of record degrades the correlations very considerably, just as in the snowpack analysis shown in Fig. 9. Possible equatorial SST–summer rainfall relationships were also explored using other ENSO indices, such as Niño-3.4 and Niño-4 describing equatorial SST anomalies to the west of the Niño-3 region, but the Niño-3 time series yielded the highest correlations.

The mature phase of a canonical ENSO cycle occurs in the early part of the year, and most ENSO-related teleconnections occur during the cold season. Annual values of bimonthly (Jan/Feb) Niño-3 values are plotted

TABLE 2. Correlation between anomalies of Niño–3 SST (an average over the box delineated by 5°N, 90°W, 5°S, and 150°W) and Jul + Aug precipitation time series shown in Figs. 7a–c, for the 30-yr period 1961–90. First row in the table gives the half-year lag correlations between winter (Jan/Feb) Niño–3 values and subsequent Jul + Aug precipitation; second row gives simultaneous correlations between Jul/Aug SST and Jul + Aug precipitation.

	Jul + Aug precipitation regions		
	I (Arizona)	II (Plains)	III (New Mexico)
Niño–3 Jan/Feb	0.07	−0.43	−0.29
Niño–3 Jul/Aug	−0.13	0.14	−0.08

in Fig. 7f, and lag correlations between this time series and the three summer precipitation regions are shown in the first row of Table 2. The best correlation is negative, implying that winter El Niño (La Niña) conditions tend to be followed by negative (positive) Plains summer rainfall anomalies. However, none of the lag correlations involving winter Niño-3 SST in Table 2 is as strong as the SWE-based lag correlation for the 1961–90 period, a point noted previously by Gutzler and Preston (1997).

Simultaneous correlations between summer Niño-3 and Southwest rainfall anomalies are much weaker—not significantly different from zero—as shown in the second row of Table 2. Summer teleconnections are known to be weak in general, as reflected in operational long-lead outlook products. As suggested by Gutzler and Preston (1997), one possible interpretation of the set of correlations shown in Table 2 is that ENSO forcing has little direct effect on summer precipitation in the Southwest, but may have an indirect lag effect via the tendency for enhanced (deficient) snowpack in the southern Rockies during El Niño (La Niña) winters.

5. Summary and discussion

An empirical orthogonal function analysis of interannual summer precipitation anomalies across the southwest United States monsoon region identified three distinct subregions of coherent variability. Seasonal rainfall fluctuations in Arizona, or the Southwest Plains of eastern New Mexico and western Texas, are separated from precipitation variability across most of New Mexico by the analysis. These patterns are not sensitive to the presence of long-term trends in the rainfall data, despite the observation that such trends are not uniform across the Southwest. Ongoing analysis of the relative importance of different forcing mechanisms that might modulate interannual variability in these subregions promises to enhance our understanding of controls on warm season precipitation.

One such control, the possible modulation of monsoon rainfall by antecedent snowpack, is examined in this paper. New Mexico precipitation exhibits an impressive negative correlation with an objective index of antecedent spring snowpack for the 1961–90 period, but this correlation does not extend to a spatially limited index of spring snow during the 1950s or early 1990s. The time series associated with the other two regions of coherent summer precipitation anomalies exhibit no correlation with antecedent spring snowpack.

These results provide some empirical evidence for spring snowpack anomalies in the southern Rockies leading summer rainfall anomalies in western New Mexico, but also indicate the limits of predictability associated with such a relationship. Collectively the results seem to imply that spring snowpack anomalies may modulate the extent to which moist monsoonal airflows penetrate into the North American continent, but from this analysis we find no evidence for snowpack exerting a significant influence on summer rainfall in those parts of the southwestern United States closer to oceanic moisture sources.

More comprehensive characterization of snowpack would enhance the analysis presented in this paper, but such data are scarce. A simple snapshot of snow conditions at the beginning of April is by itself certainly unsatisfactory for operational long-range prediction purposes. During the current year (1999), for example, snowpack in the southern Rockies was extremely deficient on 1 April 1999, consistent with expectations of anomalously low winter/spring precipitation in this region associated with cold La Niña ocean surface temperatures in the tropical Pacific (Molles and Dahm 1990; Table 2). A series of late spring snowstorms in April and May brought runoff and soil moisture conditions close to seasonal normals, however, reducing the confidence that might be placed in a summer precipitation forecast based on 1 April land surface conditions.[1]

The temporal stationarity of the spring snow–summer seasonal rainfall relationship is also questionable and needs more study. Recent analyses have suggested that decade-scale variability seated in the Pacific Ocean may modulate shorter-term seasonal fluctuations. Mo and Paegle (2000) propose that atmospheric circulation anomalies modulating Southwest summer rainfall may be associated with different combinations of tropical and extratropical Pacific SST anomalies. Higgins and Shi (2000) relate summer rainfall to variations of the Pacific Decadal Oscillation or PDO (Mantua et al. 1997). Both of these analyses emphasize the potential role played by the fluctuations of the North Pacific Ocean circulation that are not directly tied to equatorial ENSO-related SST anomalies.

Consideration of longer timescales leads naturally to the question of long-term droughts. As mentioned in section 3, a severe drought in the 1950s depressed precipitation in both winter and summer across the eastern portion of the analysis domain examined in this paper. Higgins and Shi (2000) point out that the drought period in the Southwest occurred during a negative phase of the PDO.

The various mechanisms that might trigger or act to maintain multiyear droughts are still being worked out, but land surface forcing on such timescales is often thought to act locally as a positive feedback on drought conditions. A dry land surface provides little moisture to the atmosphere via evapotranspiration, causing drought to persist (Shukla and Mintz 1982). If, as in

[1] U.S. hydrological observations are disseminated on the Internet by the NOAA National Weather Service. SWE anomaly maps for 1999 come from the National Operational Hydrologic Remote Sensing Center at http://www.nohrsc.nws.gov, and runoff and soil moisture anomaly maps come from the Climate Prediction Center at http://www.cpc.ncep.noaa.gov.

these studies, precipitation is principally limited by the supply of water vapor, then land surface anomalies can be expected to have an effect on precipitation opposite the effect postulated in this analysis.

Similarly, the local albedo feedback of snow and ice cover is a strong positive feedback on temperature in climate models in both high latitudes [at the edge of ice sheets, as proposed 30 years ago by Budyko (1969) and Sellers (1969)] and in arid regions (Charney et al. 1977). Thus different physical mechanisms linking land surface conditions with atmospheric moisture, stability, and circulation could lead to opposite relationships between land surface anomalies and rainfall. Determining the broader climatic conditions under which land surface forcing acts as a negative feedback process, as suggested by the results presented in this paper, versus as a positive feedback, will be a challenging problem for future climate dynamics research.

An empirical analysis like this one cannot definitively establish cause and effect. It is likely that spring snowpack and summer rainfall are mutually correlated with other varying components of the climate system, such as midlatitude Pacific Ocean variability, as suggested by Higgins and Shi (2000) and Mo and Paegle (2000). Forcing–response relationships can potentially be tested using numerical model simulations of the Southwest North American climate system forced by prescribed land surface anomalies, or other possible forcing functions, after such models are shown to simulate the summer precipitation climatology across the Southwest with reasonable fidelity. Achieving such fidelity has proven to be very difficult (Stensrud et al. 1995). Such modeling will help to ascertain more clearly the potential predictability of summer season rainfall anomalies.

Acknowledgments. This research has been supported by the U.S. National Science Foundation and Los Alamos National Laboratory. Chris Pacheco (U.S. Natural Resources Conservation Service) provided the snow data. P. Fawcett, D. Henderson, K. Redmond, and E. Small provided helpful comments on the manuscript. Undergraduate research assistants F. Hren and M. Duran (UNM) carried out several of the calculations.

REFERENCES

Adams, D. K., and A. C. Comrie, 1997: The North American monsoon. *Bull. Amer. Meteor. Soc.,* **78,** 2197–2213.

Barnett, T. P., L. Dümenil, U. Schlese, E. Roeckner, and M. Latif, 1989: Effects of Eurasian snow cover on regional and global climate variations. *J. Atmos. Sci.,* **46,** 661–685.

Blanford, H. F., 1884: On the connexion of Himalayan snowfall and seasons of drought in India. *Proc. Roy. Soc. London,* **37,** 3–22.

Budyko, M. I., 1969: The effects of solar radiation on the climate of the earth. *Tellus,* **21,** 611–619.

Carleton, A. M., D. A. Carpenter, and P. J. Weser, 1990: Mechanisms of interannual variability of the southwest United States summer rainfall maximum. *J. Climate,* **3,** 999–1015.

Cayan, D. R., 1996: Interannual climate variability and snowpack in the western United States. *J. Climate,* **9,** 928–948.

——, M. D. Dettinger, H. F. Diaz, and N. E. Graham, 1998: Decadal variability of precipitation over western North America. *J. Climate,* **11,** 3148–3166.

Charney, J., W. Quirk, S. Chow, and J. Kornfield, 1977: A comparative study of the effects of albedo change on drought in semiarid regions. *J. Atmos. Sci.,* **34,** 1366–1385.

Douglas, M. W., R. A. Maddox, K. Howard, and S. Reyes, 1993: The Mexican monsoon. *J. Climate,* **6,** 1665–1667.

Gutzler, D. S., and J. W. Preston, 1997: Evidence for a relationship between spring snow cover and summer rainfall in New Mexico. *Geophys. Res. Lett,* **24,** 2207–2210.

Hahn, D. J., and J. Shukla, 1976: An apparent relationship between Eurasian snow cover and Indian monsoon rainfall. *J. Atmos. Sci.,* **33,** 2461–2462.

Higgins, R. W., and W. Shi, 2000: Dominant factors responsible for interannual variability of the summer monsoon in the southwestern United States. *J. Climate,* **13,** 759–776.

——, Y. Yao, and X.-L. Wang, 1997: Influence of the North American monsoon system on the U.S. summer precipitation regime. *J. Climate,* **10,** 2600–2622.

——, K. C. Mo, and Y. Yao, 1998: Interannual variability of the United States summer precipitation regime. *J. Climate,* **11,** 2582–2606.

Horel, J. D., 1981: A rotated principal component analysis of the interannual variability of the Northern Hemisphere 500 mb height field. *Mon. Wea. Rev.,* **109,** 2080–2092.

IPCC, 1998: *The Regional Impacts of Climate Change—An Assessment of Vulnerability.* Cambridge University Press, 517 pp.

Kripalani, R. H., and A. Kulkarni, 1999: Climatology and variability of historical Soviet snow depth data: Some new perspectives in snow-Indian monsoon teleconnections. *Climate Dyn.,* **15,** 475–489.

Mantua, N. J., S. R. Hare, Y. Zhang, J. M. Wallace, and R. C. Francis, 1997: A Pacific interdecadal climate oscillation with impacts on salmon production. *Bull. Amer. Meteor. Soc.,* **78,** 1069–1079.

Mo, K. C., and J. N. Paegle, 2000: Influence of sea surface temperature anomalies on the precipitation regimes over the southwest United States. *J. Climate,* **13,** 3588–3598.

Mock, C. J., 1996: Climatic controls and spatial variations of precipitation in the western United States. *J. Climate,* **9,** 1111–1125.

Molles, M. C., Jr., and C. N. Dahm, 1990: A perspective on El Niño and La Niña: Global implications for stream ecology. *J. N. Amer. Benthol. Soc.,* **9,** 68–76.

Namias, J., 1955: Some meteorological aspects of drought, with special reference to the summers of 1952–1954 over the United States. *Mon. Wea. Rev.,* **83,** 199–205.

Paegle, J., K. C. Mo, and J. N. Paegle, 1996: Dependence of simulated precipitation on surface evaporation during the 1993 United States summer floods. *Mon. Wea. Rev.,* **124,** 345–361.

Richman, M. B., 1986: Rotation of principal components. *J. Climatol.,* **6,** 293–335.

Schmitz, J. T., and S. L. Mullen, 1996: Water vapor transport associated with the summertime North American monsoon as depicted by ECMWF analyses. *J. Climate,* **9,** 1621–1634.

Sellers, W. D., 1969: A climate model based on the energy balance of the earth–atmosphere system. *J. Appl. Meteor.,* **8,** 392–400.

Shukla, J., and Y. Mintz, 1982: Influence of land-surface evapotranspiration on the earth's climate. *Science,* **215,** 1498–1501.

Stensrud, D. J, R. L. Gall, S. L. Mullen, and K. W. Howard, 1995: Model climatology of the Mexican monsoon. *J. Climate,* **8,** 1775–1794.

——, and K.-M. Lau, 1998: Influences of sea surface temperature and ground wetness on the Asian summer monsoon. *J. Climate,* **12,** 3230–3246.

——, ——, and M. Sankar-Rao, 1996: Precursory signals associated with the interannual variability of the Asian summer monsoon. *J. Climate,* **9,** 949–964.

Yasunari, T., A. Kitoh, and T. Tokioka, 1991: Local and remote responses to excessive snow mass over Eurasia appearing in the Northern spring and summer climate—A study with the MRI GCM. *J. Meteor. Soc. Japan,* **69,** 473–486.